ELSEVIER

Journal of Non-Crystalline Solids 191 (1995) 193–199

JOURNAL OF
NON-CRYSTALLINE SOLIDS

Density of amorphous Si_xGe_{1-x} alloys prepared by high-energy ion implantation

K. Laaziri [a], S. Roorda [a,*], J.M Baribeau [b]

[a] *Groupe de recherche en physique et technologie des Couches Minces, Département de physique, Université de Montréal, CP 6128 succ. centre-ville, Montréal, Québec H3C 3J7, Canada*

[b] *National Research Council Canada, Institute for Microstructural Sciences, Ottawa K1A 0R6, Canada*

Received 28 November 1994; revised manuscript received 9 March 1995

Abstract

The atomic density of amorphous Si_xGe_{1-x} alloys ($0 \leqslant x \leqslant 1$), has been measured. The amorphous alloys were made by high-ion-energy implantation into monocrystalline Si_xGe_{1-x} layers, deposited epitaxially on silicon substrates. During the bombardments, a steel contact mask was used to create alternating lines of amorphous and crystalline material. The ratio between the densities of crystalline and amorphous alloys was measured with 0.1–0.2% accuracy using surface profilometry and Rutherford backscattering spectrometry in conjunction with channelling. Amorphous pure elements and alloys are less dense by 1.5–2.1% than the crystalline pure elements and alloys. By comparing both the amorphous and crystalline densities with Vegard's law, it is found that this law underestimates the a-Si_xGe_{1-x} densities by the same amount as those of c-Si_xGe_{1-x}.

1. Introduction

Many basic properties of amorphous Si_xGe_{1-x} alloys are not known despite mounting technological and scientific interest. For example, the atomic densities of crystalline Si_xGe_{1-x} alloys are well known [1], but some confusion exists regarding those of the amorphous alloys. The density of pure amorphous silicon, prepared by ion implantation, has recently been measured accurately [2] and it was found to be $1.8 \pm 0.1\%$ less than that of crystalline Si. Since both silicon and germanium are fourfold-coordinated covalently bonded solids and since they are completely miscible, it may be expected that the density difference between the amorphous and crystalline phases of Ge and Si_xGe_{1-x} alloys shows a similar behaviour. Early measurements of the density of deposited amorphous Ge [3] indicated a density 1% greater than crystalline Ge.

The work presented here is aimed at measuring the atomic density of a variety of amorphous Si_xGe_{1-x} alloys, prepared by ion implantation of molecular beam epitaxy (MBE) deposited monocrystalline films. Ion implantation was used for amorphization because it is known to yield void-free layers [4]. The density difference was measured using the same technique as previously used on pure Si [2], yielding similar precision.

* Corresponding author. Tel: +1-514 343 2076. Telefax: +1-514 343 6215. E-mail: roorda@lps.umontreal.ca.

0022-3093/95/$09.50 © 1995 Elsevier Science B.V. All rights reserved
SSDI 0022-3093(95)00310-X

2. Experimental procedures

2.1. Outline of experiment

The methodology of the experiment is very simple and allows the ratio of the densities of the crystalline (δ_c) and amorphous (δ_a) alloys to be determined with high precision as illustrated in Fig. 1. First, a layer of monocrystalline Si_xGe_{1-x} is deposited on a flat silicon substrate. Next, several lines on the surface (defined by a metal contact mask) are exposed to an MeV ion beam, which renders these areas amorphous. A density change upon amorphization will lead to swelling or depression of the surface, which can easily be measured by surface profilometry. In Fig. 1, this is indicated as the step height, h, at the boundary between implanted and non-implanted regions. Since the Si_xGe_{1-x} alloy is monocrystalline, the depth of the interface between the amorphous layer and the underlying crystalline alloy can be determined by ion channelling. This depth is expressed as the areal density of the amorphous region in atom/cm^2. Dividing by the crystalline density, we determined the parameter d (see Fig. 1) which is the distance between the crystalline/amorphous interface and the non-implanted surface. The ratio of the crystalline and amorphous densities is then calculated from

$$\delta_c/\delta_a = 1 + h/d. \qquad (1)$$

The error in d is mostly due to the error in the stopping power, which is estimated to be 10%. However, the error on the ratio between the crystalline and amorphous densities is not very sensitive to that in d and was estimated to be around 0.1%.

A few small corrections may be required. First, each alloy is grown epitaxially on a monocrystalline substrate. If the alloy is not completely relaxed, its density will deviate slightly from the normal value, and this has to be taken into account. Second, during the ion bombardment, small amounts of material are added (implantation) and removed (sputtering). The following section describes in detail the sample preparation, measurement techniques and correction procedures.

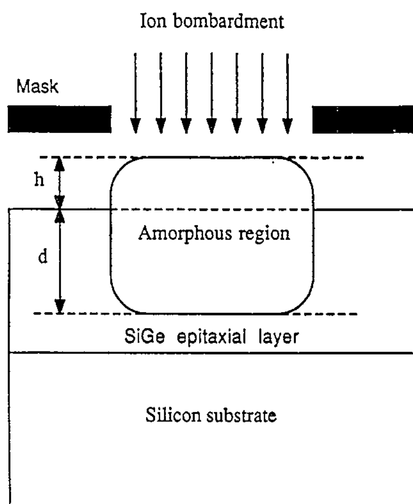

Fig. 1. Sketch of the sample after implantation, indicating: d is the original thickness of the amorphized Si_xGe_{1-x} before implantation; h is the step height.

2.2. Sample preparation

2.2.1. Deposition

The crystalline samples consisted of 2.8–3.3 μm thick Si_xGe_{1-x} layers with a Si concentration, x, ranging from 0 to 1, deposited epitaxially on silicon substrates. In addition, pure Si and Ge samples were investigated. All epitaxial layers were grown by molecular beam epitaxy (MBE) in a VG Semicon V80 system [5]. Growth was performed on lightly doped 100 mm (100) Si Czochralski wafers at a temperature of 500 ± 50°C and growth rate of $\simeq 0.5$ nm/s. The substrate preparation consisted of a 50 min treatment in a UV-ozone photo-reactor to remove surface hydrocarbons prior to loading in the growth chamber. The surface oxide was then removed in vacuum by a 600 s heat treatement at 900°C under a small Si flux (0.01 nm/s).

Double-axis diffraction measurements ((400) rocking curves; +, − geometry) of the Si/Si_xGe_{1-x} heterostructure were recorded on a Phillips MRD instrument (Cu Kα radiation) equipped with a four-crystal Bartels monochromator (resolution 12 arcsec) and a two-crystal Bonse–Hart analyzer (resolution 12 arcsec). The rocking curves for the different samples are displayed in Fig. 2. They exhibit a sharp Bragg peak due to the diffraction from the substrate crystal and a broad peak due to the epitaxial layer.

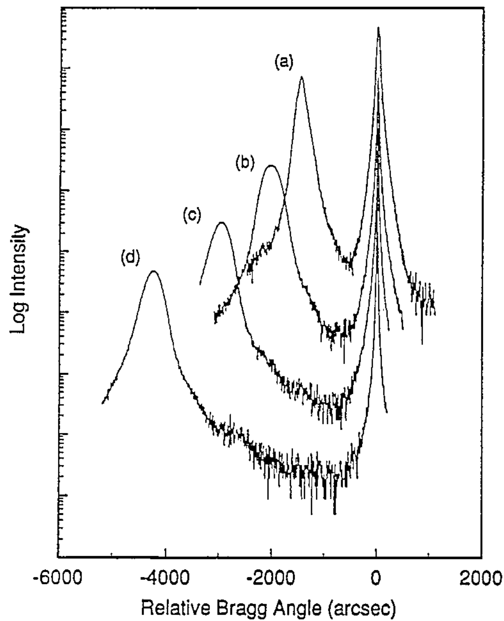

Fig. 2. (400) double-axis rocking curves for the different Si_xGe_{1-x}/Si heteroepitaxial layers: (a) $Si_{0.75}Ge_{0.25}$, (b) $Si_{0.65}Ge_{0.35}$, (c) $Si_{0.50}Ge_{0.50}$ and (d) $Si_{0.25}Ge_{0.75}$.

The composition of the various Si_xGe_{1-x} alloys was determined from the angular position of the epitaxial layer peak in the rocking curves, assuming that the layer is fully relaxed (see Table 1).

We have performed Rutherford backscattering spectrometry (RBS) of 3.0 MeV He to verify the composition and thickness, and the results are plotted in Fig. 3. Concentrations estimated by RBS are listed in Table 1. Comparing the values for x measured by X-ray diffraction and RBS, it is seen that all values agree except those for $Si_{0.85}Ge_{0.15}$. This implies that all other layers are fully relaxed. Indeed, the rocking curve for $Si_{0.85}Ge_{0.15}$ (curve (a) in Fig. 2) shows a relatively sharp peak instead of a broad bump, indicating the absence of dislocations. It may be noted that the only epitaxial layer that has not fully relaxed is the one with the lattice parameter closest to that of the Si substrate.

Table 1
Composition of the Si_xCr_{1-x} alloy determined by XRD and RBS; the values of the thickness measured by RBS are also listed

Composition, x		Thickness (μm)
XRD	RBS	
0.75	0.85	2.9
0.65	0.66	2.8
0.50	0.48	2.8
0.25	0.24	3.3

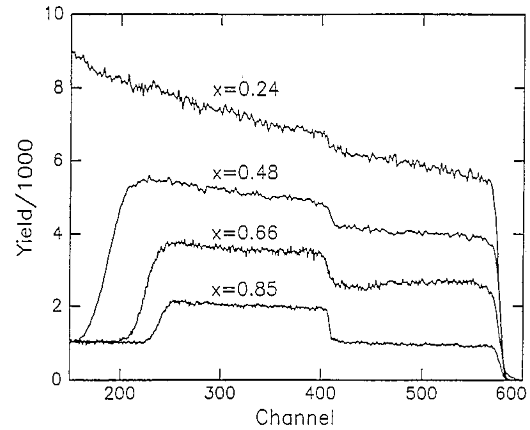

Fig. 3. Random RBS spectra for amorphous Si_xGe_{1-x} alloys.

The fully relaxed layers have the same density as bulk Si_xGe_{1-x} alloys of the same composition, but this is not true for the strained layer $Si_{0.85}Ge_{0.15}$. The in-plane compressive strain leads to an expansion in the vertical direction, but not enough to compensate fully for the compression. Therefore, a small correction must be applied to the crystalline density, and the bulk volume is

$$(a+\delta l)\times\left(a\delta l(1-P)^2/2P\right), \qquad (2)$$

where a is the lattice parameter, P is the Poisson ratio (0.278 for Si) and δl is the difference between the lattice parameter of strained and unstrained bulk. The correction to the crystalline density of the non-relaxed $Si_{0.85}Ge_{0.15}$ alloy is given by the difference between the volume of the strained and unstrained bulk; it is 0.67%.

2.2.2. Implantation

The preparation of amorphous alloys and pure elements was performed by MeV ion implantation using a 6 MV Van De Graaff tandem accelerator. We have used $^{28}Si^{2+}$ and $^{74}Ge^{2+}$ ions to different doses and energies from 2 to 2.75 MeV (see Table 2). During the implantations, a raster scan was used to achieve laterally homogeneous implantations over a 1×1 cm^2 aperture. The beam current on target never exceeded 100 nA, corresponding to a total

Table 2
Implantation parameters

Sample	Energy (MeV)	Dose (atom/cm^2)
Si	2	5×10^{15} Si^{2+}
$Si_{0.85}Ge_{0.15}$	2	5×10^{15} Si^{2+}, 5×10^{15} Ge^{2+}
$Si_{0.66}Ge_{0.34}$	2	5×10^{16} Si^{2+}
$Si_{0.48}Ge_{0.52}$	2	6×10^{16} Si^{2+}
$Si_{0.24}Ge_{0.76}$	2.75	4×10^{16} Si^{2+}
Ge	2.5	6×10^{15} Ge^{2+}

power on target of the order of 0.1 W, to avoid heating effects. Two identical samples were clamped to a copper block which was tilted by 7° to ensure that no channelling occurred during bombardment. A steel mask was clamped to one of the samples, in order to produce alternating amorphous/crystalline Si_xGe_{1-x} regions. The copper block was held at liquid nitrogen temperature, and the pressure during bombardment was typically less than 10^{-6} Torr. In one case, a mixed silicon and germanium implantation was used to avoid stoichiometry change of the alloy. For the other alloys, only silicon bombardments were performed, which led to a change in stoichiometry of less than 1%. Under the implantation conditions described above, the material will amorphize. In fact, the dose used (see Table 2) exceeds the threshold for amorphization by about a factor of five. Visual inspection and Raman spectroscopy (not shown) confirmed amorphization of the samples.

During implantation material was added by implantation, and material was removed by sputtering. To estimate how much was removed from the pure elements, we used the sputtering theory of Sigmund [6]. For the Si_xGe_{1-x} alloys, we used an approximative model which estimates Y_{SiGe}, the total sputtered yield of Si and Ge removed per ion during the bombardments,

$$Y_{SiGe} = xY_{Si} + (1-x)Y_{Ge}. \quad (3)$$

Here,

$$Y_{Si} = 0.042\,\alpha_1 S_n(E)/U_{Si} \quad (4)$$

is the partial sputtered yield of silicon of the Si_xGe_{1-x} alloy during Si^{2+} implantation, and

$$Y_{Ge} = 0.042\,\alpha_2 S_n(E)/U_{Ge} \quad (5)$$

is the partial sputtered yield of germanium of the Si_xGe_{1-x} alloy during Si^{2+} implantation. The values of the constants are $\alpha_1 = 0.25$, $\alpha_2 = 0.48$, $U_{Si} = 7.83$ eV, and $U_{Ge} = 7.63$ eV [6]. $S_n(E)$ is the nuclear energy loss of MeV silicon in the Si_xGe_{1-x} alloy, estimated by Bragg's rule [7]. The amount of sputtered material was 10% of the material added during implantation. All values are listed in Table 3.

The ratio of amorphous and crystalline densities can then be calculated using the corrected formula (1):

$$\delta_c/\delta_a = 1 + (h-a+s)/(d-a+s), \quad (6)$$

where a is the material added (implantation) and s the material removed (sputtering).

2.3. Analysis techniques

A Dektak 3030ST instrument was used to carry out the surface profilometry. Typically, three lateral

Table 3
Amorphous and crystalline densities of pure silicon, germanium and Si_xGe_{1-x} alloys; also listed are h and d parameters and their deviations.

Sample	d (10^3 nm)	h (nm)	Material added (nm)	Material sputtered (nm)	Crystalline density [a] δ_c (g/cm^3)	δ_c/δ_a	Amorphous density δ_a (g/cm^3)
Si	2.4 ± 0.2	40 ± 2	1	0.1	2.327	1.0164 ± 0.0010	2.289
$Si_{0.85}Ge_{0.15}$	2.2 ± 0.2	50 ± 2	2	0.1	2.861 [b]	1.021 ± 0.002	2.802
$Si_{0.66}Ge_{0.34}$	2.2 ± 0.2	57 ± 4	12	0.5	3.457	1.020 ± 0.002	3.389
$Si_{0.48}Ge_{0.52}$	2.2 ± 0.19	46 ± 4	13	0.6	4.009	1.015 ± 0.0010	3.947
$Si_{0.24}Ge_{0.76}$	2.63 ± 0.2	53 ± 3	9	0.1	4.694	1.0168 ± 0.0017	4.617
Ge	1.78 ± 0.18	28 ± 2	1.4	1	5.326	1.0155 ± 0.0019	5.244

[a] Ref. [1].
[b] The corrected density value of the strained layer using Eq. (5).

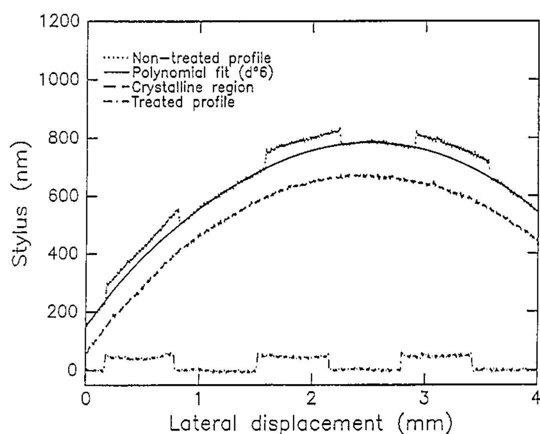

Fig. 4. Treated and non-treated Dektak profiles of $Si_{0.85}Ge_{0.15}$ alloy.

scans of 4 mm covering three periods of alternating amorphous/crystalline Si_xGe_{1-x} regions were realized at low speed (0.1 mm/s). The traces present a large curvature, which is a result of the stress induced by the implantation added to the initial curvature of the sample. The profiles were treated mathematically by subtracting a polynomial function to compensate for the curvature of the sample.

Ion channelling of 3.0 MeV $^4He^+$ ions, backscattered over 157.5° was utilized to determine the position of the amorphous/crystalline interface. The areal density of the amorphous zone was calculated using the stopping power of the Si_xGe_{1-x} alloys, deduced from Bragg's rule [8]. For Ge, the Ziegler stopping power [9] was used, and for Si the stopping power given by Santry and Werner [10,11]. The parameter d was then obtained by dividing the measured areal density by the atomic density of the crystalline Si_xGe_{1-x} alloy.

3. Results

Fig. 4 shows the surface profile of the masked region of the $Si_{0.85}Ge_{0.15}$ alloy, and a scan of the crystalline region of the same sample. The curvature of the implanted region is due to the initial curvature of the sample and stress induced by the implantation. Note that the curvature of the samples are the same before and after bombardment. Elevated regions correspond to amorphous zones. The average step height, deduced from the treated profile, is determined from 12 steps; it was found to be (50 ± 2) nm. The error on the step height is the variance in the 12 measurements. Because the amorphous alloys are laterally confined by the adjacent unimplanted regions, essentially all density change is accommodated by viscous flow. Therefore no correction for lateral expansion is required and h reflects the expansion.

Fig. 5 shows the aligned (solid circles) and non-aligned (open circles) backscattering spectra for the $Si_{0.85}Ge_{0.15}$ sample. The surface channels for Si and Ge are indicated in the figure. The discontinuity in the yield of backscattered particles around channel 250 corresponds to the interface between the $Si_{0.85}Ge_{0.15}$ layer and the Si substrate. The channeled spectrum (taken in the ⟨100⟩ direction) coincides almost completely with the random one. However, a decreased yield in the channelled spectrum can be observed in the channel range 220–320. The transition region between reduced and non-reduced channelled yield, indicated with an arrow, identifies the position of the interface separating the amorphized $Si_{0.85}Ge_{0.15}$ alloy and the underlying undamaged c-$Si_{0.85}Ge_{0.15}$. The position of this interface is consistent with an amorphous $Si_{0.85}Ge_{0.15}$ areal density of $(1.09 \pm 0.10) \times 10^{19}$ atom/cm^2. This would correspond to an equivalent c-$Si_{0.85}Ge_{0.15}$ thickness (d in Fig. 1) of (2.2 ± 0.2) μm. The error is mainly due to

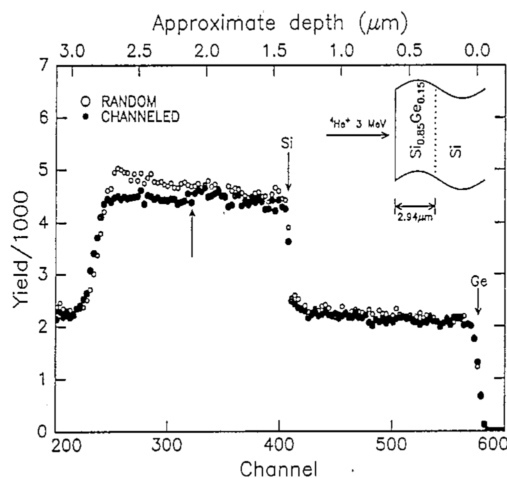

Fig. 5. Channelled and random RBS spectra for amorphous $Si_{0.85}Ge_{0.15}$ alloy: full circles: ⟨100⟩ channelled; open circles: random spectrum. The depth scale is based on a surface approximation calculation, and for backscattering from Ge only.

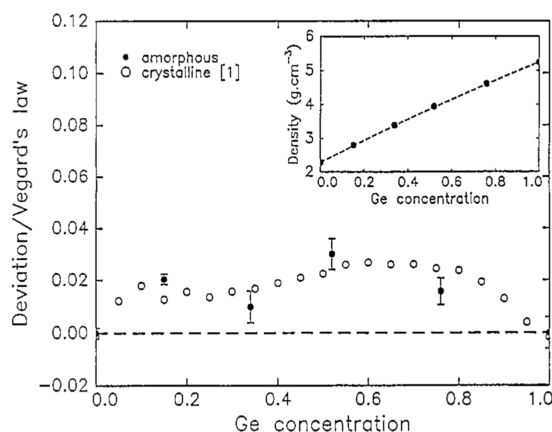

Fig. 6. Difference between measured density and density predicted by Vegard's law for both crystalline and amorphous Si_xGe_{1-x} alloys. The density according to Vegard's law has been calculated separately for the amorphous (full circles) and crystalline (open circles) alloys. Inset: measured a-Si_xGe_{1-x} densities (points) and density according to Vegard's law (dashed line).

the uncertainty in the stopping power, but also contains contributions from energy straggling, counting statistics and detector resolution. Using theses values for h and d, and with the appropriate corrections, the ratio δ_c/δ_a is found to be (1.021 ± 0.002). The results for all the alloys are listed in Table 3.

4. Discussions

It has been argued that, unlike crystalline alloys, amorphous alloys can accommodate differences in atomic size of constituent elements. Mössbauer spectroscopy of local structure in Fe-based alloys supported this suggestion [12]. Such an effect would imply the existence of a density difference between amorphous and crystalline alloys that depends on stoichiometry. In order to evaluate our results in this context, we have compared our density measurements and literature values for c-Si_xGe_{1-x} alloys with the values predicted by Vegard's law [1]. Fig. 6 shows the deviation between the measured density (points) relative to Vegard's law (dashed line). It should be noted that Vegard's law has been evaluated separately for crystalline and amorphous alloys; shown in the figure is the difference between the measured density and that predicted by the corresponding Vegard curve. We have observed that both crystalline and amorphous densities show positive deviations from Vegard's law. We can also see that both amorphous and crystalline Si_xGe_{1-x} alloys are less dense than predicted by Vegard's law. The magnitude of the difference appears to be the same within the errors for the amorphous and the crystalline alloys.

For the crystalline alloys, it has been suggested [13] that the deviations from Vegard's law are due to the difference in compressibility of Si and Ge (1.000×10^{12} cm^2/dyn for Si, 1.333×10^{12} cm^2/dyn for Ge), i.e. the partial inability of the crystalline alloy to accommodate atomic size differences. The present observation of similar deviations from Vegard's law in a-Si_xGe_{1-x} alloys shows that, for this system, the amorphous alloys do not accommodate atomic size differences with more ease than the crystalline alloys. The present result is markedly different from the earlier observation [12] that atomic size differences can be more easily accommodated in amorphous metal alloys than in their crystalline counterparts. It may be noted that in our case the system is a semiconductor alloy whose behaviour is apparently dominated by the stiffness and directionality of the covalent bond. Calculations of the elastic properties of a continuous random network model, based on the Keating potential, showed that the bulk modulus of a-Ge is 3% less than that of c-Ge [14]. A similar calculation showed that a-Si is softer than c-Si [14]. If the softening upon amorphization would be the same in Si and Ge, the deviation from Vegard's law would be the same for the amorphous and crystalline alloys.

5. Conclusions

Both amorphous alloys and pure elements are less dense than crystalline alloys and pure elements. Differences range from 1.5% for $Si_{0.48}Ge_{0.52}$ to 2.1% for $Si_{0.85}Ge_{0.15}$. It was found that Vegard's law underestimates both the amorphous and the crystalline Si_xGe_{1-x} density by the same amount which indicates that amorphization-induced softening is similar in Si and Ge and Si_xGe_{1-x} alloys.

It is a pleasure to acknowledge L. Cliche for help with RBS and ion implantation, P. Berichon and R. Gosselin for expert technical assistance. The authors wish to thank R.W. Cochrane for useful discussions. This work is financially supported by the Natural Science and Engineering Research Council of Canada (NSERC) and the Fonds pour la formation de Chercheurs et l'Aide a la Recherche (FCAR). One author (K.L.) would like to thank the Agence Canadienne pour le Développement International (ACDI) for financial assistance.

References

[1] J.P. Dismukes, L. Ekstrom and R.J. Paff, J. Phys. Chem. 68 (1964) 3021.
[2] J.S. Custer, M.O. Thompson, D.C. Jacobson, J.M. Poate, S. Roorda, W.C. Sinke and F. Spaepen, Appl. Phys. Lett. 64 (1994) 437.
[3] T.M. Donovan, E.J. Ashley and W.E. Spicer, Phys. Lett. 32A (1970) 85.
[4] D. Williamson, S. Roorda, M. Chicoine, R. Tabti, P.A. Stolk, S. Acco and F.W. Saris, Appl. Phys. Lett. 67 (1995) 226.
[5] J.-M. Baribeau, T.E. Jackman, D.C. Houghton, P. Maigné and M.W. Denhoff, J. Appl. Phys. 63 (1988) 5738.
[6] P. Sigmund, Phys. Rev. B184 (1969) 383.
[7] J.F. Ziegler, J.P. Biersack and U. Littmark, The Stopping and Ranges of Ions in Solids (Pergamon, Oxford, 1985).
[8] J.W. Mayer, and E. Rimini, Ion Beam Handbook for Material Analysis (Academic Press, New York, 1977).
[9] J.F. Ziegler, He Stopping Powers and Ranges in all Elemental Matter (Pergamon, New York, 1978).
[10] D.C. Santry and R.D. Werner, Nucl. Instr. Meth. 159 (1979) 523.
[11] D.C. Santry and R.D. Werner, Nucl. Instr. Meth. 178 (1980) 523.
[12] A.M. van der Kraan and K.H.J. Buschow, Phys. Rev. B27 (1983) 2693.
[13] J. Friedel, Philos. Mag. 46 (1955) 514.
[14] L. Guttman, Solid State Commun. 24 (1977) 212.